Check for updates

Current Status of Carbon-Related Defect Luminescence in GaN

Friederike Zimmermann, Jan Beyer, Christian Röder, Franziska C. Beyer, Eberhard Richter, Klaus Irmscher, and Johannes Heitmann*

Highly insulating layers are a prerequisite for gallium nitride (GaN)-based power electronic devices. For this purpose, carbon doping is one of the currently pursued approaches. However, its impact on the optical and electrical properties of GaN has been widely debated in the scientific community. For further improvement of device performance, a better understanding of the role of related defects is essential. To study optically active point defects, photoluminescence is one of the most frequently used experimental characterization techniques. Herein, the main recent advances in the attribution of carbon-related photoluminescence bands are reviewed, which were enabled by the interplay of a refinement of growth and characterization techniques and state-of-the-art first-principles calculations developed during the last decade. The predicted electronic structures of isolated carbon defects and selected carbon-impurity complexes are compared to experimental results. Taking into account both of these, a comprehensive overview on the present state of interpretation of carbon-related broad luminescence bands in bulk GaN is presented.

1. Introduction

Gallium nitride (GaN) has become an indispensable compound semiconductor due to its numerous applications in opto-[1,2] and microelectronic[3,4] devices. GaN-based light emitting diodes and laser diodes show higher efficiencies than competing materials and, by alloying with Al or In, the bandgap can cover both the visible and UV spectral range.[5] In addition, AlGaN/GaN heterostructures lead to the formation of a 2D electron gas (2DEG) at the AlGaN/GaN interface, which enables high-frequency switching devices.[6,7] Furthermore, due to the large breakdown voltage and thermal stability, GaN is the perfect candidate for high-power applications.[8,9]

As a prerequisite for GaN-based power electronic devices, highly insulating buffers are required.[10,11] Here, carbon doping plays a major role to compensate for donor impurities, which occur even in nominally undoped GaN films. However, the role of carbon-related defects in heterojunction field effect transistors is multiple. They were shown to play a major role in the buffer transport mechanisms generally[12] and to contribute to current collapse[13,14] as well as a dynamical shift of the threshold voltage[11,15] in the devices.

Advancements in the field of GaN growth resulted in bulk material of improved structural quality, often with dislocation densities below 10^6 cm^{-2}.[16,17] As a consequence, the influence of point defects as a limiting factor of device performance is gaining importance.[18–20] Therefore, a better understanding of point defects in GaN is required to improve device performance further and to control unwanted side effects.

To study optically active point defects in semiconductors, photoluminescence (PL) is one of the experimental techniques most frequently used. The impact of carbon on the luminescence properties is, without doubt, one of the most debated subjects related to point defects in GaN. Although those discussions reach back more than 40 years,[21] considerable progress in the understanding of carbon-related point defect levels was made in the last decade.

Two main factors greatly improved the understanding of carbon-related defect levels in GaN. On one hand, the implementation of hybrid functionals in density functional theory (DFT) accounts for carrier localization at acceptor species. This led to vast changes in the predicted energy values of charge state

F. Zimmermann, J. Beyer, C. Röder, J. Heitmann
Institute of Applied Physics
TU Bergakademie Freiberg
Leipziger Str. 23, 09599 Freiberg, Germany
E-mail: f.zimmermann@physik.tu-freiberg.de

F. C. Beyer
Department Materials
Fraunhofer Institute for Integrated Systems and Device Technology IISB
Schottkystrasse 10, 91058 Erlangen, Germany

E. Richter
Ferdinand-Braun-Institut gGmbH
Leibniz-Institut für Höchstfrequenztechnik
Gustav-Kirchhoff-Str. 4, 12489 Berlin, Germany

K. Irmscher
Department of Volume Crystals
Leibniz-Institut für Kristallzüchtung
Max-Born-Straße 2, 12489 Berlin, Germany

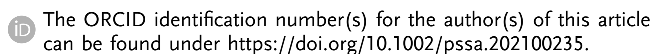
The ORCID identification number(s) for the author(s) of this article can be found under https://doi.org/10.1002/pssa.202100235.

© 2021 The Authors. physica status solidi (a) applications and materials science published by Wiley-VCH GmbH. This is an open access article under the terms of the Creative Commons Attribution License, which permits use, distribution and reproduction in any medium, provided the original work is properly cited.

DOI: 10.1002/pssa.202100235

© 2021 The Authors. physica status solidi (a) applications and materials science published by Wiley-VCH GmbH

transition levels, which required a revision of long-standing experimental interpretations. On the other hand, recent improvements in bulk material quality, especially doping control and homogeneity,[16] facilitate interpretation of optical spectra. The occurrence of fine structures on the high-energy wing of broad emission bands allows us to distinguish between PL transitions of close or equal peak energies.

For a detailed compilation of early work on point-defect-related PL transitions in GaN, the reader is referred to the comprehensive review published by Reshchikov and Morkoç in 2005.[22] In this review, the until then identified PL bands in GaN are described and a detailed summary of their behavior, e.g., dependence on temperature, excitation power density, and doping, is given. Emanating from the importance of C doping for optoelectronic devices and the fact that luminescence methods are more and more often applied for device analysis,[11,23–27] in this article we focus on the recent progress with respect to understanding the role of C in bulk GaN. Accordingly, we will emphasize the defect-related radiative transitions in the visible spectral region of carbon-doped bulk GaN. Complementary findings, derived both experimentally and by first-principles calculations, will be included to complete the picture.

This article is structured according to the type of carbon-related defect center involved. First, the effect of single C atoms occupying GaN lattice sites as well as the effect of increasing C concentration is discussed. Starting from introducing transitions related to C occupying the N site (Section 2.1), the effect of an increasing C concentration on the PL spectra is addressed (Section 2.2) as well as the possibility of C incorporation on the Ga site (Section 2.3). Second, the formation of point defect complexes containing C and residual impurities (Sections 3.1 and 3.2) as well as multicarbon complexes (Section 3.3) and their impact on PL spectra are considered. Finally, the results are summarized.

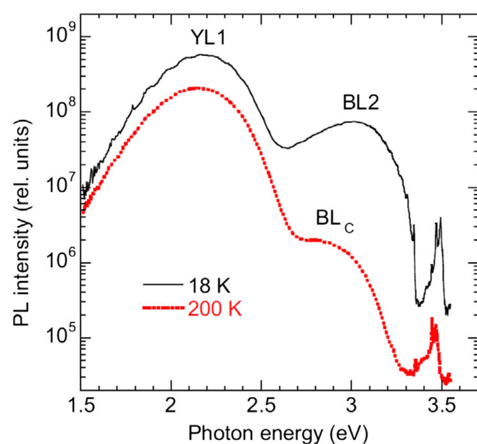

Figure 1. Typical steady-state PL spectra of bulk GaN:C at 18 and 200 K excited at 325 nm with $P_{exc} = 0.2\,W\,cm^{-2}$. The transition at $E_{max} = 2.2$ eV denoted as YL1 is related to the C_N acceptor level. At 18 K, BL2 at $E_{max} = 3.0$ eV is predominant in the blue spectral region and originates from transitions via the $C_N - H_i$ deep donor level. At 200 K BL2 is thermally quenched and BL_C at $E_{max} = 2.9$ eV is recorded. BL_C is proposed to be the secondary transition of YL1 via the C_N donor level. Reproduced with permission.[84] Copyright 2018, American Physical Society.

2. Luminescence of Single Carbon Defects

Typical PL spectra of highly resistive carbon-doped GaN, recorded under above-bandgap excitation (325 nm/3.815 eV) at 18 and 200 K, are shown in **Figure 1**. Apart from the near-band-edge emission above 3.4 eV, three broad defect-related PL bands can be observed. To precisely refer to specific defect-related PL bands with close energies, the nomenclature proposed in Reshchikov et al.[28] for PL bands in nominally undoped GaN is used whenever applicable. Here, YL1 at $E_{max} = 2.2$ eV is the most intense transition at 18 and 200 K. In addition, at 18 K a blue luminescence band around $E_{max} = 3.0$ eV can be observed that is denoted as BL2. At 200 K, BL2 is thermally quenched and another blue band at $E_{max} = 2.9$ eV, BL_C, is revealed.

The properties of the most likely C-related YL1, BL_C, and BL2 are described in detail in Section 2.1 and 3.2, respectively. They should not be confused with the following similar PL bands of different origin: in the blue spectral region BL1 around $E_{max} = 2.9$ eV with a zero-phonon line (ZPL) at 3.10 eV is often observed in nominally undoped GaN grown by hydride vapor phase epitaxy (HVPE) and metalorganic chemical vapor deposition (MOCVD) and is associated with Zn impurities.[28] In the yellow spectral region YL3 with $E_{max} = 2.10$ eV and a ZPL at 2.36 eV is tentatively proposed to originate from a transition metal impurity found in n-type GaN grown by HVPE.[29,30]

2.1. Low C Concentration: Carbon on N Site – C_N

Carbon in GaN is expected to preferentially occupy the N lattice site due to similar atomic radii. This is reflected by predicted C_N formation energies of 1.0 – 2.0 eV in n-type GaN[31–34] compared to values above 5.0 eV in the case of C_{Ga} and C_i formation[31–34] and further supported experimentally.[35] Early first-principles calculations based on DFT predicted the substitutional C_N defect to be a shallow acceptor.[36,37] However, these early calculations were commonly performed in the framework of Local density approximation (LDA) and generalized gradient approximation (GGA), which are known to suffer from a severe underestimation of the bandgap and do not take into account possible carrier localization around acceptor species. Considerable improvement was achieved by the implementation of hybrid functionals. First-principles calculations using the Heyd–Scuseria–Ernzerhof (HSE) functional, which was shown to reliably describe the electronic structure of solids, now consistently find the C_N acceptor level much deeper in the GaN bandgap due to strong hole localization.[32,38] Numerous reports applying different parameters to the HSE approach consistently predicted the C_N acceptor level in the range between 0.9 and 1.1 eV above the valence band maximum (VBM, E_V).[31,33,34,38,39]

This is in good agreement with experimental findings of a thermally activated reduction in the resistivity of carbon-doped GaN with an activation energy $E_A = (0.95 \pm 0.10)$ eV.[40–43] Furthermore, the acceptor nature of the main defect in carbon-doped bulk GaN was recently verified by the observation of p-type conductivity that was thermally activated with $E_A = 1.02$ eV.[41,44] The calculated acceptor level also agrees with the properties of the commonly observed H1 hole trap at $E_V + 0.85$–0.90 eV analyzed by deep level transient spectroscopy (DLTS) or minority carrier transient spectroscopy[45–52] and the

© 2021 The Authors. physica status solidi (a) applications and materials science published by Wiley-VCH GmbH

optical level of an electron trap at about 3.0 eV below the conduction band minimum associated with an optical threshold at ≈2.6 eV as determined from steady-state photocapacitance, pulsed photoionization, or deep level optical spectroscopy.[45,46,53–55] Several studies found those traps not only to be associated with carbon but also with the yellow luminescence around 2.2 eV.[47,56–58]

2.1.1. Yellow Luminescence and the C_N Acceptor Level: YL1

The yellow luminescence has been observed in GaN grown by various methods, including microcrystals formed by a direct reaction of molten Ga with NH_3,[21] molecular beam epitaxy (MBE),[59–61] MOCVD,[28,62,63] and HVPE.[28,64,65] Early studies concerned with the yellow band around 2.2 eV in GaN already pointed to a possible relation to carbon contamination.[21,66] Based on the aforementioned first theoretical predictions for C_N forming a shallow acceptor level, it was commonly assumed that yellow luminescence was caused by Ga vacancies (V_{Ga}) or their complexes.[21,67–70] In addition, transitions involving structural defects,[71,72] nitrogen vacancies (V_N)[73] (later revised, e.g., in Glaser et al.[74]), and Ga interstitials Ga_i[74] were discussed as the possible origin. Furthermore, a relation to the donor incorporation was reported, e.g., for oxygen[61,75,76] and silicon.[19,77–79]

However, taking the further development of the theoretical approaches into account, C_N is a suitable candidate for the yellow luminescence. Configuration-coordinate (CC) diagrams that consider not only the thermodynamic transition level but also atomic relaxations were calculated from the DFT-predicted parameters.[32] As shown in **Figure 2**, a PL band with a ZPL at $E_0 = 2.60$ eV and a peak maximum at 2.14 eV was suggested.[32] Furthermore, resonant absorption is expected to peak around 2.95 eV.

This agrees very well with the experimental findings that are displayed in **Figure 3**.[21] The authors of this early work found the yellow luminescence to peak at 2.15 eV and measured a characteristic excitation band with a maximum around 3.15 eV. As this characteristic excitation strongly overlaps with the GaN fundamental absorption, the fitting by a Gaussian function may result in an overestimation of its peak energy position. Nevertheless,

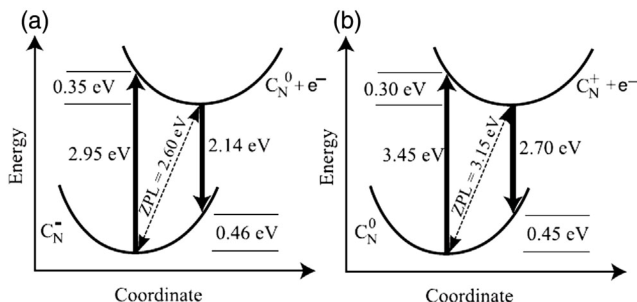

Figure 2. Configuration-coordinate diagrams for the C_N impurity in GaN calculated by DFT using the HSE hybrid functional. a) If electrons in the conduction band recombine with a neutral C_N^0, the emission associated with the $C_N^0 + e^- \rightarrow C_N^-$ transition is predicted to occur with a peak at 2.14 eV. b) If one takes into consideration the C_N donor level (+/0), then electrons in the conduction band may recombine with positively charged C_N^+. The emission associated with the $C_N^+ + e^- \rightarrow C_N^0$ transition is predicted to peak at 2.7 eV. Reproduced with permission.[32] Copyright 2014, American Physical Society.

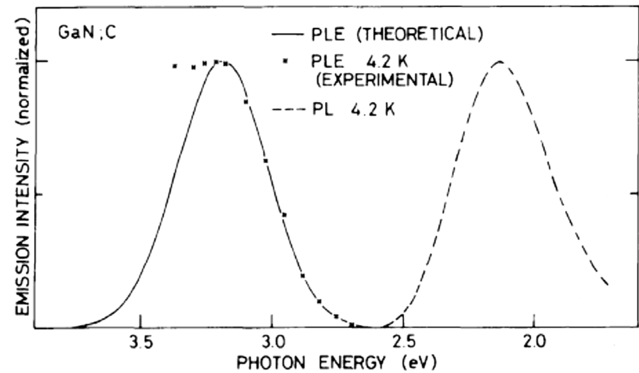

Figure 3. PL (broken line) and characteristic excitation band (solid line) obtained from the PLE spectrum (squares) of the yellow luminescence of C-doped GaN, taken at 4.2 K. The position of the ZPL is estimated to be (2.64 ± 0.05) eV. Reproduced with permission.[21] Copyright 1980, The Physical Society of Japan and The Japan Society of Applied Physics.

the value $E_0 = 2.64$ eV calculated from the intercept of the excitation and emission band is in remarkably good agreement with the value of 2.60 eV predicted for the ZPL of C_N.

In later publications, the nomenclature YL1[28,80] was introduced to differentiate the C_N-related PL from other luminescence bands in the same spectral region. YL1 is characterized by an asymmetric peak shape with a steeper high-energy side compared to the low-energy side. However, this band shape is frequently influenced by a strong overlap of the YL1 with other emission bands in the blue, green, and red spectral region. In particular, the sharp emission onset around 2.6 eV is often obscured by green emission in HVPE-grown GaN.[42,43]

Nevertheless, recent improvement of bulk material quality enabled the direct observation of the ZPL in PL measurements. This is shown exemplarily in **Figure 4** by data obtained from an undoped bulk GaN sample grown by HVPE. At low temperatures, the ZPL related to the shallow donor–acceptor–pair (DAP) recombination was found at $E_0 = 2.57$ eV in undoped GaN grown by HVPE and MOCVD,[80] accounting for only 1% of the peak intensity. At ≈40 K the ZPL related to the free-electron-to-acceptor (e,A) recombination clearly emerged at 2.59 eV. Based on those values, Reshchikov et al. derived the thermodynamic transition level of C_N to be at $E_V + 0.916$ eV.[80]

In nominally undoped n-type GaN, YL1 thermally quenches above 400–450 K with an activation energy $E_A = (900 \pm 50)$ meV[21,80,81] that is in agreement with the value expected for thermal emission of holes from the C_N acceptor level to the valence band. Apparent activation energies in the range between 0.06 eV for conductive n-type GaN and 1.8 eV for highly resistive GaN have been reported. In the case of n-type GaN, the thermal quenching behavior is determined by the lifetime of YL1 that, for (e, A) transitions, is inversely proportional to the electron concentration. The apparent very high activation energies determined from semi-insulating GaN can be explained by the model of abrupt and tunable thermal quenching.[81–83] If those effects are properly accounted for, $E_A = (900 \pm 50)$ meV can be confirmed.[81]

Furthermore, a hole capture coefficient of $C_{pA1} = (3.7 \pm 1.6) \times 10^{-7} cm^3 s^{-1}$[29,80,84] was determined from

© 2021 The Authors. physica status solidi (a) applications and materials science published by Wiley-VCH GmbH

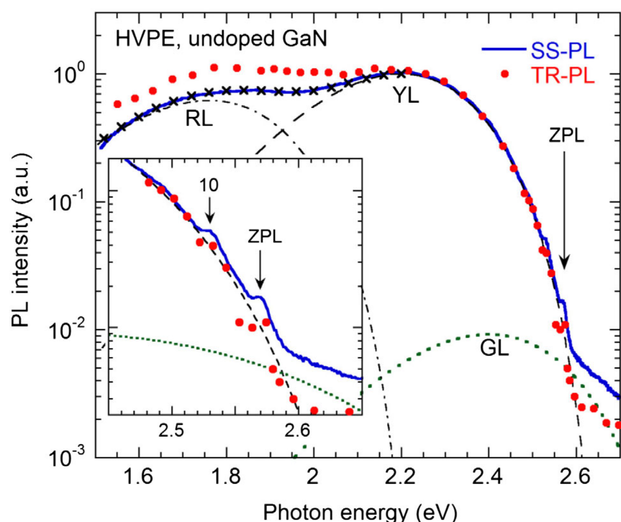

Figure 4. Normalized PL spectrum at $T = 18$ K from undoped bulk GaN grown by HVPE. The solid line is the steady-state PL spectrum, denoted by SS-PL. The dotted, dashed, and dash–dotted lines are calculated contributions of the GL, YL, and RL bands, respectively. The × symbols show the sum of the calculated YL and RL bands. The filled circles are the time-resolved PL spectrum taken 1 ms after a laser pulse. The inset shows a zoomed-in spectrum near the ZPL, where even the first phonon replica, denoted by 10, is discernible. Reproduced with permission.[80] Copyright 2016, American Physical Society.

the thermal quenching of YL1 in n-type GaN. From time-resolved PL measurements, the electron capture coefficient of $C_{nA1} = (1.1 \pm 0.1) \times 10^{-13} \text{cm}^3\,\text{s}^{-1}$ was derived.[28,29,80,84]

Thus, the thermodynamic transition level of the defect responsible for YL1, estimated to be at ≈0.9 eV above the VBM from the ZPL energy as well as from the thermal quenching, is in good agreement with both the predicted acceptor level of C_N and the energy of the H1 hole trap analyzed by DLTS. Especially for low unintentionally doped high-quality GaN grown by HVPE and MOCVD, a remarkable accordance between the overall carbon concentration determined by secondary ion mass spectrometry (SIMS) and the H1 hole trap concentration has been found.[51,52]

2.1.2. Blue Luminescence and the C_N Donor Level: BL_C

Interestingly, HSE-based DFT calculations additionally predict a C_N donor level at energies of $E_V + 0.25$–0.48 eV.[32–34,85,86] This donor level can be expected to be observed by PL only after the acceptor level is saturated with (photogenerated) holes, which is the case either for high excitation power densities or in highly compensated material, where a considerable portion of the C_N centers are already in the neutral charge state in the dark.

Initially, the green luminescence band commonly observed in HVPE-grown GaN (later labeled GL1[28]) was proposed to originate from this secondary C_N-related transition.[85] However, based on a C-doping study of MOCVD-grown GaN, Lesnik at el. suggested a blue luminescence band around 2.92 eV to be this secondary transition.[87] Later Reshchikov et al.[84] revised their attribution to GL1 and reported a detailed characterization of a PL band around 2.85 eV, labeled BL_C, that exhibits the predicted properties. In n-type GaN codoped by Si and C, BL_C emerged at high excitation power densities, when the YL1 was observed to saturate. Over a large set of such samples, these two luminescence bands were found to correlate.[84] In semi-insulating samples, BL_C was detected at much lower excitation power densities.

Although no direct observation of the respective ZPL has been reported yet, the ZPL was estimated to be at $E_0 = (3.2 \pm 0.1)$ eV from a fit of the BL_C band shape.[84] The experimentally determined parameters are in close agreement with of Lyons et al.[32] and Reshchikov et al.[84] (cf. Figure 2b). From E_0, the donor level was estimated to be at $E_V + (0.3 \pm 0.1)$ eV. Compared to the charge carrier capture coefficients of other defects responsible for major defect-related PL bands in GaN, this defect level is characterized by an unexpectedly small hole and a large electron capture coefficient of $C_{pA2} \approx 1 \times 10^{-10} \text{cm}^3\,\text{s}^{-1}$ and $C_{nA2} \approx 1 \times 10^{-9} \text{cm}^3\,\text{s}^{-1}$,[84] respectively. Accordingly, its radiative recombination efficiency is very low.

Considering the dependence on C concentration and excitation power density, the blue luminescence analyzed at room temperature in several recent publications might likely be associated with BL_C.[63,88,89] However, BL_C is easily confused with a Zn-related blue luminescence band BL1 around 2.9 eV[28] and, at low temperatures, usually obscured in semi-insulating GaN by the 3.0 eV PL band BL2, which is attributed to $C_N - H_i$ complexes (see Section 3.2 for more details). BL_C can most reliably be identified by time-resolved PL measurements at very short delays after a laser pulse (1–10 ns)[84] because it decays much faster than BL1 ($\tau \approx 10-100\,\mu$s)[28] and BL2 ($\tau \approx 0.4\,\mu$s).[90]

Additional experimental evidence for a carbon-related donor level was provided by observation of a trap at $E_V + 0.29$ eV by DLTS in p-type GaN:Mg codoped with C.[49] This trap closely followed the carbon concentration, together with the H1 hole trap. Thus, the authors inferred that both traps have a common chemical origin, namely, C_N. They concluded from this observation that C_N not only compensates electrons in n-type GaN but also holes in p-type GaN. Fang et al. observed trapping by two charge states of C_N to be a major hole-trapping process in n-type HVPE-grown GaN by transient absorption spectroscopy.[91] The hole capture coefficient derived for C_N^+ (BL_C) amounts to $C_{pA2} \approx 8.7 \times 10^{-7}\,\text{cm}^3\,\text{s}^{-1}$ and thus is considerably larger than the value determined from PL.[84] The hole capture coefficient determined for C_N^- (YL1; cf., Figure 2a) $C_{pA1} \approx 1.6 \times 10^{-6}\,\text{cm}^3\,\text{s}^{-1}$ and the electron capture coefficient determined for C_N^+ (BL_C; cf., Figure 2b) $C_{nA2} \approx 7.6 \times 10^{-9}\,\text{cm}^3\,\text{s}^{-1}$ agree well with PL results.[84]

To sum up, there is a remarkable accordance between the theoretically predicted properties of C_N and the experimentally derived characteristics of YL1. The detection of BL_C and its correlation to YL1 in a variety of samples further supports the assignment of YL1 to the C_N acceptor level while BL_C is proposed to be the secondary luminescence band related to the C_N donor level.

2.2. Medium C Concentration: PL Quenching

To identify the impurities possibly related to certain luminescence bands, concentration series were typically investigated, for carbon doping reported, in previous studies.[41–43,61,63,85,87,92,93]

© 2021 The Authors. physica status solidi (a) applications and materials science published by Wiley-VCH GmbH

The discussion regarding the assignment of YL1 to carbon-related defects was preserved by recurring publications that found no correlation between the PL band intensity and the C concentration.[61,79]

However, the often forwarded assumption that a higher concentration of an impurity or dopant species results in an increase of the corresponding PL bands has to be considered carefully. First, it was shown that in GaN the intensity of PL associated with a specific defect saturates at rather low defect concentrations, typically in the range of $10^{16}\,cm^{-3}$ (determined on HVPE-grown bulk GaN).[58]

Second, this assumption does not take into account the possibility of dopant incorporation in the form of different competing defect species. The defect formation is also expected to be highly sensitive to the growth conditions used. As an example, it was shown that for MOCVD growth the C incorporation can be controlled by minority carrier injection (achieved by above-bandgap illumination).[94,95] Usually for GaN grown by MOCVD, the YL1 intensity is observed to increase with the carbon concentration, at least up to the range of low $10^{18}\,cm^{-3}$.[63,85,87,92] However, when grown under above-bandgap illumination, a decrease of YL1 proportional to the illumination power was found, although the total C concentration determined by SIMS was not affected by the illumination.[94] It was concluded by Kaess et al.[94] that C was incorporated in a configuration different from C_N^-.

Further evidence for the need to consider C incorporation in other configurations was given by recent works on highly resistive HVPE-grown GaN.[41–43,93] HVPE is inherently carbon-free, resulting in low residual carbon concentrations in nominally undoped HVPE-grown GaN. Accordingly, no YL1 was detected in nominally undoped reference samples. In HVPE-grown GaN with intentional carbon doping a strong yellow emission was observed.[42,43,93] Additionally, when the carbon concentration was increased from low $10^{17}\,cm^{-3}$ to $1 \times 10^{18}\,cm^{-3}$ Zvanut et al. observed the emergence of a blue luminescence band around 2.95 eV, which they ascribed to BL_C. However, no correlation of YL1 to the carbon concentration was observed.[42,43,93]

Instead, especially for carbon concentrations above mid-$10^{18}\,cm^{-3}$, the overall luminescence intensity strongly decreases, indicating the formation of nonradiative defects. Simultaneously, the apparent peak maximum in the yellow spectral region continously shifts to higher energies.[42,93] This apparent peak shift was proposed to be related to two overlapping PL bands. Whereas Zvanut et al.[42] suggested the involvement of carbon complexes, Zimmermann et al.[93] associated the apparent peak shift with a pronounced decrease of YL1 intensity revealing an underlying green emission. The latter was attributed to GL2, which has been proposed to be related to V_N.[96,97]

A comparison to electrical data indicates that in the case of elevated C concentrations, centers compensating for the C_N acceptor are incorporated.[41,43,44] These groups observed that for C concentrations above high $10^{18}\,cm^{-3}$ the electrical resistivity is saturating or even decreasing again. In particular, a detailed analysis by Piotrzkowski et al. of the compensation ratio of the C_N acceptor indicated an almost equal amount of donor species incorporated when the carbon concentration exceeds mid-$10^{18}\,cm^{-3}$.[44] Apart from C interstitials, they proposed C occupying the Ga site as the most plausible donor candidate, while Richter et al. concluded its predominant incorporation in tricarbon complexes[43] (cf., Section 3.3).

In summary, the overall PL intensity is typically found to quench for high carbon concentrations. This points not only to the formation of nonradiative defects, but also indicates the incorporation of carbon in forms different from C_N.

2.3. High C Concentration: Carbon on Ga Site – C_{Ga}

Because C_{Ga} is predicted to behave as a shallow donor,[32,33,36] for high doping concentrations a self-compensation mechanism was proposed.[36,98] The formation energy of C_{Ga} strongly decreases when the Fermi level approaches the valence band.[31–33,38,99] In fact, a theoretical study investigating the carbon incorporation under typical conditions of metalorganic vapor phase epitaxy found the Fermi level to be pinned between 1.25 and 1.60 eV at growth conditions where the formation energies of C_N and C_{Ga} are similar.[99] Consequently, the incorporation of C_{Ga} in equal concentration to C_N is predicted for carbon concentrations above $\approx 5 \times 10^{17}\,cm^{-3}$.[99] A recent annealing study of intrinsically (by adjustment of the growth conditions) C-doped GaN grown by MOCVD provided evidence for the incorporation of C_{Ga}[100] at high C doping concentrations. Xu et al. interpreted an increase of V_{Ga} defects after thermal annealing (1000 °C) of a GaN sample with carbon concentration above $10^{19}\,cm^{-3}$ as the result of migration of C atoms from the Ga to the N site. This was supported by an increase in YL1 intensity after thermal annealing.[101] The conversion was observed to start between 700 °C and 800 °C, which roughly agrees with a predicted C migration starting at temperatures above 900 K (627 °C).[102] The same group also pointed out that the doping sources likely influence the lattice sites of incorporated C, as no increase in V_{Ga} defects was found for GaN doped by propane.[101]

Based on the early GGA and LDA-predicted shallow C_N acceptor level, blue luminescence bands in C-doped GaN are sometimes proposed to originate from DAP-type transitions between the C_{Ga} donor level and the C_N acceptor level.[46,57,88,98,103,104]

Regarding the considerably deeper nature of the C_N acceptor level derived by state-of-the-art first-principles calculations (see Section 2.1), this attribution should be revised. The luminescence band around 3.0 eV detected in GaN grown by MOCVD and HVPE might be associated with the C_N-H_i-related BL2. Detailed information concerning BL2 is given in Section 3.2. Blue luminescence around 2.85 eV is more likely associated with the Zn-related BL1[28] or BL_C (cf., Section 2.1.2).

Thus, although high C concentrations are expected to favor the formation of C_{Ga}, considering the present understanding of C-related point defects, no luminescence bands that can be related to C_{Ga} have been reported yet.

In summary, C_N is predicted to be the dominant carbon-related defect over a wide range of concentrations.[105] However, in the case of high C concentrations experiments indicate that different C configurations need to be considered.

© 2021 The Authors. physica status solidi (a) applications and materials science published by Wiley-VCH GmbH

3. Luminescence of Carbon-Containing Defect Complexes

Depending on the particular growth technique, many other chemical elements may be introduced into the growing GaN bulk crystal. Most abundant are O, Si, and H.[106] Two main carbon-impurity complexes have been considered to be responsible for broad PL bands in GaN. The first one is the $C_N - O_N$ complex, which was initially discussed as one possible origin of the yellow luminescence.[31,85,107] The second one is $C_N - H_i$, which is proposed to be responsible for a metastable blue luminescence band around 3.0 eV labeled as BL2.[84,108]

3.1. An Early Candidate for Yellow Luminescence: $C_N - O_N$

Due to its general abundance, oxygen is a common impurity in GaN growth regardless of the growth method. Occupying the N site in the GaN crystal lattice, it acts as a shallow donor and contributes significantly to the residual n-type conductivity of nominally undoped GaN.[109] In an n-type material the formation energy of $C_N - O_N$ predicted by first-principles calculations is comparable to the C_N formation energy[105] or even higher by about 1.5 eV.[108,110] However, the formation energy of C_N increases when the Fermi level approaches midgap. As a consequence, the formation of $C_N - O_N$ is found favorable over the formation of isolated C_N for Fermi levels ranging from the VBM to ≈2.1 eV above the VBM.[105,108,110] $C_N - O_N$ is predicted to be a deep donor with its (0/+) charge state transition level at $E_V + 0.75$ eV and a much deeper (+/2+) charge state transition level at $E_V + 0.14$ eV by these groups. The calculated CC diagram shown in **Figure 5** proposes an absorption maximum at 3.30 eV and a PL maximum at 2.25 eV. Those parameters are in fair agreement with the properties of the YL1. Despite the predicted second donor level, no secondary PL band is expected for $C_N - O_N$ because of the electrostatic repulsion of the positively charged second donor level and the photoexcited holes. Based on those predictions and the missing evidence of a secondary PL band, the $C_N - O_N$ complex was proposed to be responsible for the yellow luminescence around 2.2 eV in samples containing a considerable amount of O[31,85] and C_N was proposed to be responsible for yellow luminescence around 2.1 eV in samples of high purity

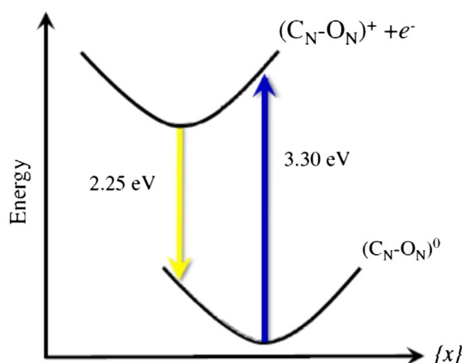

Figure 5. Configuration-coordinate diagram of $(C_N - O_N)^0$ complex illustrating optical absorption and emission energies. Reproduced with permission.[31] Copyright 2013, American Physical Society.

where GL1 (commonly observed in HVPE-grown GaN[28]) was thought to be the secondary band.[85]

However, neutral deep donors (e.g., $C_N - O_N$) are expected to capture photoexcited holes less efficiently than ionized deep acceptors (e.g., C_N^-). Consequently, PL related to $C_N - O_N$ should be weak in n-type GaN.

Furthermore, C_N and O_N are next nearest neighbours and the binding energy of those complexes is expected to be comparatively low. In fact, Christenson et al. estimated the ratio $[C_N - O_N]/[C_N]$ to be orders of magnitude smaller than 1 over a wide range of oxygen concentrations,[110] as shown in **Figure 6** (according to the calculations of Christenson et al. a similar argument holds for the concentration of $C_N - Si_{Ga}$; cf., Figure 6).

This means that even for oxygen concentrations in the range of 1×10^{19} cm^{-3} the majority of C is expected to be incorporated in the form of isolated C_N. This is further supported by a recent Fourier-transform infrared spectroscopy (FTIR) analysis of local vibrational modes (LVMs) in C-doped GaN grown by MOCVD.[35] Wu et al. analyzed two LVMs whose intensity correlated with the C concentration. By comparing their wavenumbers and polarization dependence to first-principles predictions, they obtained best agreement for the configuration C_N^-. Even for C concentrations $> 10^{19}$ cm^{-3} LVMs predicted for $C_N - O_N$ could not be observed, indicating a low concentration of the complex.

In line with this, the previous attribution of the yellow luminescence band in MOCVD-grown GaN to the $C_N - O_N$ complex was reconsidered.[80,84] In fact, the detection of the YL1-related ZPL as well as BL_C can be seen as evidence for the C_N-related YL1 being the dominant contribution to PL in the yellow spectral region also in MOCVD-grown samples.

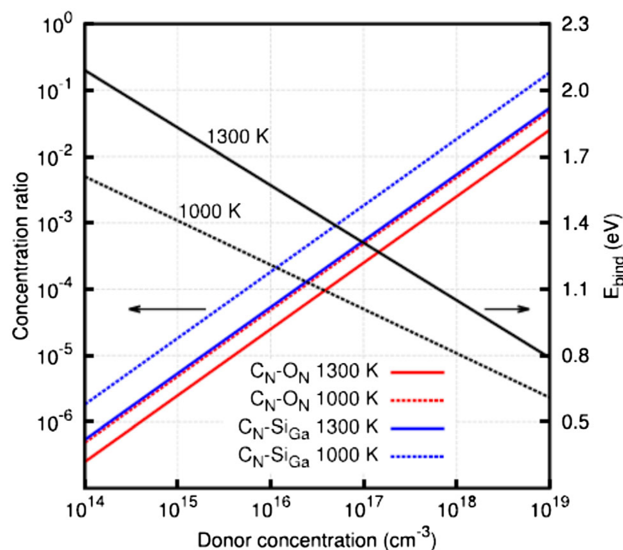

Figure 6. The concentration ratio of C_N–donor complexes to the total concentration of C_N, $[C_N\text{–Donor}]/[C_N]$ for O_N and Si_{Ga} donors in GaN (left vertical axis) and the complex binding energy (right vertical axis) required for the ratio to be unity as a function of the donor concentrations, obtained from a detailed balance analysis of complex formation and dissociation reactions. Two growth temperatures (1000 and 1300 K) were considered. Reproduced with permission.[110] Copyright 2015, AIP Publishing LLC.

© 2021 The Authors. physica status solidi (a) applications and materials science published by Wiley-VCH GmbH

Thus, although the optical transitions predicted for $C_N - O_N$ seem to be in reasonable agreement with the experimentally determined properties of the yellow luminescence, based on the previous discussion its attribution to C_N is much more likely.

3.2. Metastable Blue Luminescence BL2 in Semi-Insulating GaN: $C_N - H_i$

Another frequent impurity is hydrogen. Interstitial hydrogen is predicted to act as a donor for Fermi levels below 3.0 eV.[105,108] The formation of complexes between C_N^- and H_i^+ can be expected from the attractive nature of the Coulomb interaction. First-principles calculations find the formation energy of $C_N - H_i$ complexes to be around 3.0 eV in n-type material.[105,108] If the Fermi level is close to the C_N acceptor level the incorporation of $C_N - H_i$ is found to be favorable over the incorporation of C_N.[105,108] The $C_N - H_i$ complex is predicted to be a deep donor with its (0/+) charge state transition level between 0.1 and 0.3 eV above the valence band edge.[105,108]

A blue PL band around 3.0 eV labeled BL2 is often observed in highly resistive and semi-insulating GaN grown by MOCVD and HVPE.[90,108,111–114] At low temperatures, BL2 can be distinguished from other PL bands in the blue spectral region by its high-energy fine structure that is highlighted in **Figure 7**.

The ZPL at 3.33 eV is accompanied by phonon replicas at multiples of 91 meV, the GaN LO-phonon mode,[115] and multiples of 36 meV corresponding to a (pseudo) local vibrational mode.[90,108] BL2 quenches at temperatures above 75 K with $E_A \approx$ 140–150 meV.[84,90,114] This value agrees well with the thermodynamic transition level ≈150 meV above the VBM as determined from the ZPL.[90,108]

BL2 bleaches under continuous UV exposure, whereas the YL1 band rises simultaneously, as shown in **Figure 8**.[43] The original state can be restored after the material is kept in the dark at room temperature for several hours to days.[108,116] The

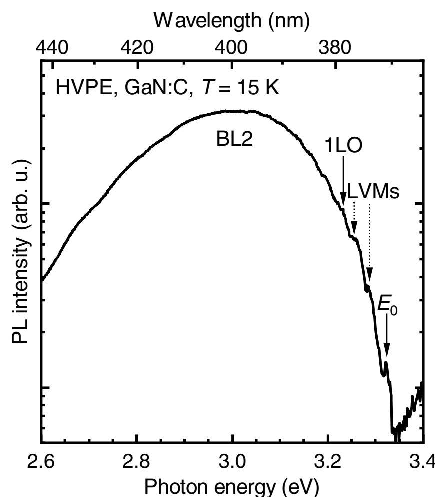

Figure 7. Low-temperature ($T = 15$ K) PL spectrum of carbon-doped bulk GaN ([C] = 5×10^{17} cm^{-3}) grown by HVPE excited at $P_{exc} = 36$ mW cm^{-2}. The ZPL of the BL2 band at $E_0 = 3.323$ eV and its first LO-phonon replica are indicated with an arrow. The dashed arrows mark the first two replicas related to the LVMs at distances of 36 meV.

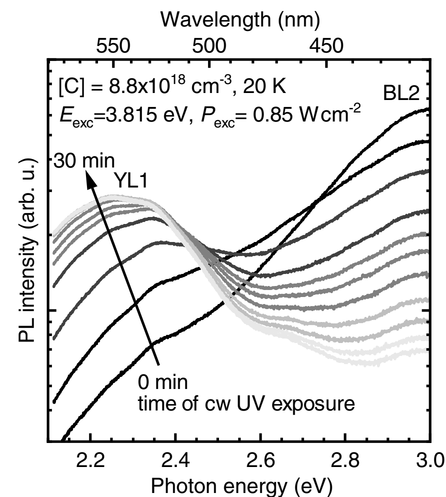

Figure 8. Above-bandgap excited PL spectrum of carbon-doped bulk GaN displaying the bleaching of BL2 and simultaneous increase of YL1 during continuous UV illumination with $P_{exc} = 0.85$ W cm^{-2}.

spectral transformation of BL2 to YL1 indicates a conversion of the defect responsible for BL2 into the YL1 center.[90,108,111–114] It was therefore proposed,[90,108] that BL2 originates from a complex of the YL1 center and hydrogen, which can be dissociated by a recombination-enhanced defect reaction.[117] Considering the association of YL1 to the C_N acceptor level (cf., Section 2.1), BL2 is consequently attributed to the $C_N - H_i$ complex. The thermodynamic transition level determined from the ZPL as well as the thermal quenching roughly agrees with the range of predicted $C_N - H_i$ donor energies. Furthermore, the nearly exponential decay at low temperatures with a characteristic time constant of 0.3–0.4 μs[84,90] indicates that BL2 is an internal transition between an excited hydrogen-like state close to the conduction band and the deep donor level at 0.15 eV above the VBM.

The fact that BL2 can only be observed in highly resistive and semi-insulating GaN can be explained by the complex being most stable in the range 1.0 eV $< E_F <$ 3.0 eV above the VBM, with a calculated binding energy of 1.2 eV.[105,108] Its concentration can thus be expected to be negligible in n-type material.

BL2 is only observed in GaN grown by HVPE and MOCVD, where hydrogen is an abundant impurity. The participation of hydrogen is further supported by annealing experiments in N_2 atmosphere. Annealing at 1000 °C completely supressed BL2 and YL1 was found to increase. After annealing the H concentration was reduced below the SIMS detection limit, whereas the concentration of other residual impurities was not affected.[113]

Based on the beginning transformation at temperatures between 600 °C and 700 °C, those authors estimated $E_A =$ 2.3–2.5 eV for the complex dissociation. Note that this is the sum of the binding energy of the $C_N - H_i$ complex and the migration barrier of H^+.[113] Assuming the predicted binding energy of 1.2 eV,[105,108] the estimated migration barrier of 1.1–1.3 eV is in good agreement with migration barriers predicted for the $Mg_{Ga} - H$[118] and $C_N - O_N - H$[108] complex dissociation. At room temperature, hydrogen returns to the

© 2021 The Authors. physica status solidi (a) applications and materials science published by Wiley-VCH GmbH

complex,[108] thus explaining the restoration of the initial BL2 and YL1 intensities. The process is thermally activated with $E_A \approx 1.35$ eV as determined from the temperature dependence of the recovery time.[111]

In conclusion, BL2 is a metastable luminescence band around 3.0 eV merely detected in highly resistive and semi-insulating GaN. Based on its interplay with YL1, it is associated with $C_N - H_i$.

3.3. Sub-Bandgap Excited Luminescence RL_C: Multicarbon Complexes

Just recently, the possibility of bi- and tricarbon defects started to be reconsidered theoretically. The formation of pairs formed from C_N and C_{Ga} or interstitial C configurations was investigated by two groups independently. Matsubara and Belotti[33] as well as Deák et al.[34] found formation energies for carbon pairs in the range 2.2–3.0 eV when E_F is close to the C_N acceptor level. Furthermore, Deák at al. also predicted a tricarbon defect comprising one interstitial C with two C_N ($(C-N)_N + 2C_N$) with a similar formation energy. Those values are low enough compared to the C_N formation energy to consider the possible effect of C defects containing more than one C atom on experimental findings.

In fact, the presence of tricarbon defects in bulk GaN grown by HVPE and C doped either with pentane or butane was indicated by local vibrational modes observed in infrared absorption spectroscopy.[43,119] A detailed analysis of the isotope effect on the LVMs in crystals with ^{13}C-enriched doping clearly proved the assignment of those modes to complexes involving three C atoms.[120] Based on their polarization behavior, those LVMs were proposed to be related to crystallographically inequivalent configurations of $C_N - C_{Ga,off} - C_N$ ($C_{Ga,off}$ denotes an off-center Ga site).[120] Furthermore, the intensity of these complex-related LVMs was sensitive to additional illumination with light of 385 nm (3.22 eV), indicating the presence of related charge state transition levels in the GaN bandgap.

This is further supported by the observation of an absorption onset at 2.5–2.6 eV resulting in a bulk photovoltaic effect in surface photovoltage (SPV) measurements[121] and a PL band around 1.62 eV in those samples,[93] for clarity further referred to as RL_C. RL_C is associated with an excitation onset at 2.4 eV and an excitation maximum at 2.7 eV. A similar luminescence band was earlier described for GaN doped by propane.[122] RL_C was found to follow the C concentration. Based on the emission and excitation energies as well as the thermal quenching, RL_C was proposed to be an internal transition between an effective-mass-like excited state and a deep ground state level of a deep trap associated with the tricarbon defects.[93] However, from the available data, it was not possible to determine whether the deep center is a deep donor or acceptor with the respective ground state in the lower or upper half of the bandgap.

In summary, there is increasing experimental evidence for the incorporation of multicarbon complexes that have not usually been considered in the interpretation of experimental data. It is likely that not only the optical but also the electrical properties of highly C-doped GaN are influenced by these complexes.

4. Conclusion

Carbon doping of GaN is a topic of great current interest, e.g., for creating highly resistive buffer layers of power electronic devices. Yet, the detailed identification of carbon-related defects and their influence on the material properties has been lively discussed for more than 40 years. Building on notable advances over the last decade regarding theoretical calculations, available bulk material quality, and a deeper understanding of the influence of experimental characterization conditions, an update on the current status of the particular subfield of interpretation of carbon-related luminescence bands is provided in this review.

The main respective optical transitions, assuming the C-related origin of the PL bands described previously, are summarized in the following list and visualized in the band diagram model in **Figure 9**.

YL1 Band: this luminescence band can be detected around 2.2 eV with a resonant absorption at about 3 eV. At low temperatures the ZPL related to the DAP transition can be identified at 2.57 eV. The observed optical properties and thermal quenching behavior of YL1 are in good agreement with recent DFT calculations predicting the C_N (0/−) acceptor level about 0.9 eV above the VBM.

BL_C Band: this PL band is characterized by a luminescence peak around 2.85 eV. BL_C occurs after saturation of YL1 under high excitation power densities or in semi-insulating GaN. It is proposed to be the secondary band of YL1 that is caused by transitions via the C_N (+/0) deep donor level ≈0.3 eV above the VBM after trapping of a second hole by the C_N center.

BL2 Band: This broad luminescence band observed in highly resistive and semi-insulating GaN is characterized by a peak maximum at 3.0 eV and a distinct high-energy fine structure with a ZPL at 3.33 eV. BL2 bleaches under prolonged UV illumination, whereas the YL1 intensity increases simultaneously. Based on this behavior and considering annealing experiments, BL2 is associated with transitions between a hydrogen-like excited state and the (0/+) donor of the $C_N - H_i$ complex. The activation

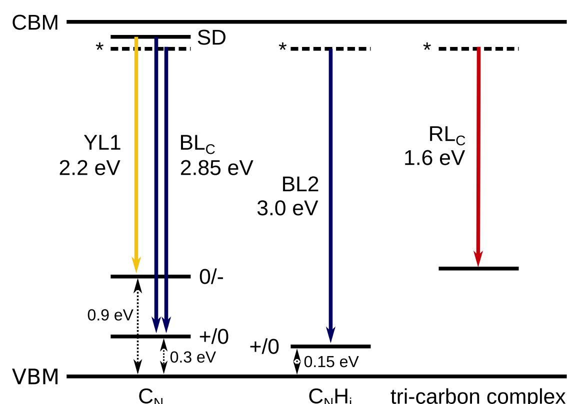

Figure 9. Schematic band diagram model summarizing the peak energies of C-related PL bands. The labels used are introduced in the text. SD denotes "shallow donors." Dashed lines annotated by an asterisk indicate excited states. Note that for the tricarbon-related PL a similar representation with an acceptor ground state in the upper half of the bandgap and an excited state close the the valence band also is suitable to explain the experimental findings.

© 2021 The Authors. physica status solidi (a) applications and materials science published by Wiley-VCH GmbH

energy of thermal quenching $E_A = 0.15$ eV lies within the range of predicted donor-level energies.

RL_C Band: The PL band at 1.62 eV revealed by sub-bandgap excitation is associated with a resonant absorption band around 2.7 eV. It is proposed to originate from an internal transition between an effective-mass-like excited state and a deep ground state level related to tricarbon complexes.

The recent progress reported in the literature was summarized and a rather consistent picture of the influence of different involved donor and acceptor levels on carbon-related PL bands could be given, including the contribution of relevant carbon-impurity complexes. Nevertheless, the richness and complexity of the interplay of growth techniques, growth conditions, dopant sources, and defect formation in GaN as well as future improvements in the theoretical treatment of point defects is certainly believed to provide further insights.

Acknowledgements

The authors benefited from collaborations and discussions with G. Gärtner, I. Gamov, I. Levine, S. Seidel, and A. Schmidt.

Open access funding enabled and organized by Projekt DEAL.

Conflict of Interest

The authors declare no conflict of interest.

Keywords

carbon, carbon complexes, GaN, luminescence

Received: April 19, 2021
Revised: July 14, 2021
Published online: August 24, 2021

[1] S. Nakamura, *Solid State Commun.* **1997**, *102*, 237.
[2] G. Li, W. Wang, W. Yang, Y. Lin, H. Wang, Z. Lin, S. Zhou, *Rep. Progr. Phys.* **2016**, *79*, 056501.
[3] H. Morkoç, S. Strite, G. Gao, M. Lin, B. Sverdlov, M. Burns, *J. Appl. Phys.* **1994**, *76*, 1363.
[4] T. J. Flack, B. N. Pushpakaran, S. B. Bayne, *J. Electron. Mater.* **2016**, *45*, 2673.
[5] D. S. Arteev, A. V. Sakharov, E. E. Zavarin, W. V. Lundin, A. N. Smirnov, V. Y. Davydov, M. A. Yagovkina, S. O. Usov, A. F. Tsatsulnikov, *J. Phys.: Conf. Ser.* **2018**, *1135*, 012050.
[6] O. Ambacher, B. Foutz, J. Smart, J. R. Shealy, N. G. Weimann, K. Chu, M. Murphy, A. J. Sierakowski, W. J. Schaff, L. F. Eastman, R. Dimitrov, A. Mitchell, M. Stutzmann, *J. Appl. Phys.* **2000**, *87*, 334.
[7] P. D. Ye, B. Yang, K. K. Ng, J. Bude, G. D. Wilk, S. Halder, J. C. M. Hwang, *Int. J. High Speed Electron. Syst.* **2004**, *14*, 791.
[8] E. A. Jones, F. F. Wang, D. Costinett, *IEEE J. Emerg. Sel. Top. Power Electron.* **2016**, *4*, 707.
[9] Y. Zhang, A. Dadgar, T. Palacios, *J. Phys. D: Appl. Phys.* **2018**, *51*, 273001.
[10] G. Meneghesso, M. Meneghini, D. Bisi, R. Silvestri, A. Zanandrea, O. Hilt, E. Bahat-Treidel, F. Brunner, A. Knauer, J. Wuerfl, E. Zanoni, *ECS Trans.* **2013**, *58*, 187.
[11] M. Huber, M. Silvestri, L. Knuuttila, G. Pozzovivo, A. Andreev, A. Kadashchuk, A. Bonanni, A. Lundskog, *Appl. Phys. Lett.* **2015**, *107*, 032106.
[12] M. J. Uren, M. Cäsar, M. A. Gajda, M. Kuball, *Appl. Phys. Lett.* **2014**, *104*, 263505.
[13] P. B. Klein, S. C. Binari, K. Ikossi, A. E. Wickenden, D. D. Koleske, R. L. Henry, *Appl. Phys. Lett.* **2001**, *79*, 3527.
[14] M. J. Uren, J. Moreke, M. Kuball, *IEEE Trans. Electron Devices* **2012**, *59*, 3327.
[15] I. Rossetto, F. Rampazzo, M. Meneghini, M. Silvestri, C. Dua, P. Gamarra, R. Aubry, M.-A. di Forte-Poisson, O. Patard, S. Delage, G. Meneghesso, E. Zanoni, *Microelectron. Reliab.* **2014**, *54*, 2248.
[16] M. Bockowski, M. Iwinska, M. Amilusik, M. Fijalkowski, B. Lucznik, T. Sochacki, *Semicond. Sci. Technol.* **2016**, *31*, 093002.
[17] *Gallium Nitride Materials and Devices XII*, Vol. *10104* (Eds: H. Fujikura, T. Yoshida, M. Shibata, Y. Otoki, In J.-I. Chyi, H. Fujioka, H. Morkoç, Y. Nanishi, U. T. Schwarz, J.-I. Shim), International Society for Optics and Photonics, SPIE, Bellingham, WA **2017**, pp. 13–20.
[18] A. Alkauskas, M. D. McCluskey, C. G. Van de Walle, *J. Appl. Phys.* **2016**, *119*, 181101.
[19] M. Bockowski, M. Iwinska, M. Amilusik, B. Lucznik, M. Fijalkowski, E. Litwin-Staszewska, R. Piotrzkowski, T. Sochacki, *J. Cryst. Growth* **2018**, *499*, 1.
[20] A. Chatterjee, S. K. Khamari, R. Kumar, S. Porwal, A. Bose, T. Sharma, *Superlattices Microstruct.* **2020**, *148* 106733.
[21] T. Ogino, M. Aoki, *Jpn. J. Appl. Phys.* **1980**, *19*, 2395.
[22] M. A. Reshchikov, H. Morkoç, *J. Appl. Phys.* **2005**, *97*, 061301.
[23] C.-H. Lin, T. A. Merz, D. R. Doutt, M. J. Hetzer, J. Joh, J. A. del Alamo, U. K. Mishra, L. J. Brillson, *Appl. Phys. Lett.* **2009**, *95*, 033510.
[24] M. Meneghini, A. Stocco, N. Ronchi, F. Rossi, G. Salviati, G. Meneghesso, E. Zanoni, *Appl. Phys. Lett.* **2010**, *97*, 063508.
[25] D. Zhou, Y. Ni, Z. He, F. Yang, Y. Yao, Z. Shen, J. Zhong, G. Zhou, Y. Zheng, L. He, Z. Wu, B. Zhang, Y. Liu, *Phys. Status Solidi C* **2016**, *13*, 345.
[26] Y. Isobe, H. Hung, K. Oasa, T. Ono, T. Onizawa, A. Yoshioka, Y. Takada, Y. Saito, N. Sugiyama, K. Tsuda, T. Sugiyama, I. Mizushima, *J. Appl. Phys.* **2017**, *121*, 235703.
[27] R. Sugie, T. Uchida, K. Matsumura, H. Sako, *J. Electron. Mater.* **2020**, *49*, 5085.
[28] M. A. Reshchikov, J. D. McNamara, M. Toporkov, V. Avrutin, H. Morkoç, A. Usikov, H. Helava, Y. Makarov, *Sci. Rep.* **2016**, *6*, 37511.
[29] M. A. Reshchikov, J. D. McNamara, H. Helava, A. Usikov, Y. Makarov, *Sci. Rep.* **2018**, *8*, 8091.
[30] M. A. Reshchikov, R. M. Sayeed, U. Özgür, D. O. Demchenko, J. D. McNamara, V. Prozheeva, F. Tuomisto, H. Helava, A. Usikov, Y. Makarov, *Phys. Rev. B* **2019**, *100*, 045204.
[31] D. O. Demchenko, I. C. Diallo, M. A. Reshchikov, *Phys. Rev. Lett.* **2013**, *110*, 087404.
[32] J. L. Lyons, A. Janotti, C. G. Van de Walle, *Phys. Rev. B* **2014**, *89*, 035204.
[33] M. Matsubara, E. Bellotti, *J. Appl. Phys.* **2017**, *121*, 195701.
[34] P. Deák, M. Lorke, B. Aradi, T. Frauenheim, *Phys. Rev. B* **2019**, *99*, 085206.
[35] S. Wu, X. Yang, H. Zhang, L. Shi, Q. Zhang, Q. Shang, Z. Qi, Y. Xu, J. Zhang, N. Tang, X. Wang, W. Ge, K. Xu, B. Shen, *Phys. Rev. Lett.* **2018**, *121*, 145505.
[36] A. F. Wright, *J. Appl. Phys.* **2002**, *92*, 2575.
[37] P. Bogusławski, E. L. Briggs, J. Bernholc, *Appl. Phys. Lett.* **1996**, *69*, 233.
[38] J. L. Lyons, A. Janotti, C. G. Van de Walle, *Appl. Phys. Lett.* **2010**, *97*, 152108.

© 2021 The Authors. physica status solidi (a) applications and materials science published by Wiley-VCH GmbH

[39] D. O. Demchenko, M. A. Reshchikov, *J. Appl. Phys.* **2020**, *127*, 155701.
[40] H. Tang, J. B. Webb, J. A. Bardwell, S. Raymond, J. Salzman, C. Uzan-Saguy, *Appl. Phys. Lett.* **2001**, *78*, 757.
[41] M. Iwinska, R. Piotrzkowski, E. Litwin-Staszewska, T. Sochacki, M. Amilusik, M. Fijalkowski, B. Lucznik, M. Bockowski, *Appl. Phys. Express* **2017**, *10*, 011003.
[42] M. E. Zvanut, S. Paudel, E. R. Glaser, M. Iwinska, T. Sochacki, M. Bockowski, *J. Electron. Mater.* **2019**, *48*, 2226.
[43] E. Richter, F. C. Beyer, F. Zimmermann, G. Gärtner, K. Irmscher, I. Gamov, J. Heitmann, M. Weyers, G. Tränkle, *Cryst. Res. Technol.* **2019**, *55*, 1900129.
[44] R. Piotrzkowski, M. Zajac, E. Litwin-Staszewska, M. Bockowski, *Appl. Phys. Lett.* **2020**, *117*, 012106.
[45] A. Hierro, D. Kwon, S. A. Ringel, M. Hansen, J. S. Speck, U. K. Mishra, S. P. DenBaars, *Appl. Phys. Lett.* **2000**, *76*, 3064.
[46] A. Armstrong, A. Arehart, D. Green, J. S. Speck, U. K. Mishra, S. A. Ringel, *Phys. Status Solidi C* **2005**, *2*, 2411.
[47] U. Honda, Y. Yamada, Y. Tokuda, K. Shiojima, *Jpn. J. Appl. Phys.* **2012**, *51*, 04DF04.
[48] T. Tanaka, K. Shiojima, Y. Otoki, Y. Tokuda, *Thin Solid Films* **2014**, *557*, 207.
[49] T. Narita, K. Tomita, Y. Tokuda, T. Kogiso, M. Horita, T. Kachi, *J. Appl. Phys.* **2018**, *124*, 215701.
[50] G. Alfieri, V. K. Sundaramoorthy, *J. Appl. Phys.* **2019**, *126*, 125301.
[51] K. Kanegae, H. Fujikura, Y. Otoki, T. Konno, T. Yoshida, M. Horita, T. Kimoto, J. Suda, *Appl. Phys. Lett.* **2019**, *115*, 012103.
[52] H. Huang, X. Yang, S. Wu, J. Shen, X. He, L. Wei, D. Liu, F. Xu, N. Tang, X. Wang, W. Ge, B. Shen, *Appl. Phys. Lett.* **2020**, *117*, 112103.
[53] A. Armstrong, C. Poblenz, D. S. Green, U. K. Mishra, J. S. Speck, S. A. Ringel, *Appl. Phys. Lett.* **2006**, *88*, 082114.
[54] E. Gaubas, T. Ceponis, J. Mickevicius, J. Pavlov, V. Rumbauskas, M. Velicka, E. Simoen, M. Zhao, *Semicond. Sci. Technol.* **2018**, *33*, 075015.
[55] E. Gaubas, P. Baronas, T. Čeponis, L. Deveikis, D. Dobrovolskas, E. Kuokstis, J. Mickevičius, V. Rumbauskas, M. Bockowski, M. Iwinska, T. Sochacki, *Mater. Sci. Semicond. Process.* **2019**, *91* 341.
[56] A. Y. Polyakov, N. B. Smirnov, E. B. Yakimov, I.-H. Lee, S. J. Pearton, *J. Appl. Phys.* **2016**, *119*, 015103.
[57] H. Yamada, H. Chonan, T. Takahashi, T. Yamada, M. Shimizu, *AIP Adv.* **2018**, *8*, 045311.
[58] M. A. Reshchikov, A. Usikov, H. Helava, Y. Makarov, V. Prozheeva, I. Makkonen, F. Tuomisto, J. H. Leach, K. Udwary, *Sci. Rep.* **2017**, *7*, 9297.
[59] R. Armitage, W. Hong, Q. Yang, H. Feick, J. Gebauer, E. R. Weber, S. Hautakangas, K. Saarinen, *Appl. Phys. Lett.* **2003**, *82*, 3457.
[60] Z.-Q. Fang, D. Look, B. Claflin, S. Haffouz, H. Tang, J. Webb, *Phys. Status Solidi C* **2005**, *2*, 2757.
[61] D. Pohl, V. Solovyev, S. Röher, J. Gärtner, I. Kukushkin, T. Mikolajick, A. Großer, S. Schmult, *J. Cryst. Growth* **2019**, *514*, 29.
[62] C. B. Soh, S. J. Chua, H. F. Lim, D. Z. Chi, S. Tripathy, W. Liu, *J. Appl. Phys.* **2004**, *96*, 1341.
[63] F. Liang, D. Zhao, D. Jiang, Z. Liu, J. Zhu, P. Chen, J. Yang, S. Liu, Y. Xing, L. Zhang, *Nanomaterials* **2018**, *8*, 1026, https://doi.org/10.3390/nano8121026.
[64] A. Hoffmann, L. Eckey, P. Maxim, J.-C. Holst, R. Heitz, D. Hofmann, D. Kovalev, G. Stevde, D. Volm, B. Meyer, T. Detchprohm, K. Hiramatsu, H. Amano, I. Akasaki, *Solid-State Electron.* **1997**, *41*, 275.
[65] M. A. Reshchikov, *Phys. Status Solidi A* **2021**, *218*, 2000101.
[66] S. O. Kucheyev, M. Toth, M. R. Phillips, J. S. Williams, C. Jagadish, G. Li, *J. Appl. Phys.* **2002**, *91*, 5867.
[67] J. Neugebauer, C. G. Van de Walle, *Appl. Phys. Lett.* **1996**, *69*, 503.
[68] K. Saarinen, T. Laine, S. Kuisma, J. Nissilä, P. Hautojärvi, L. Dobrzynski, J. M. Baranowski, K. Pakula, R. Stepniewski, M. Wojdak, A. Wysmolek, T. Suski, M. Leszczynski, I. Grzegory, S. Porowski, *Phys. Rev. Lett.* **1997**, *79*, 3030.
[69] T. Mattila, R. M. Nieminen, *Phys. Rev. B* **1997**, *55*, 9571.
[70] F. J. Xu, B. Shen, L. Lu, Z. L. Miao, J. Song, Z. J. Yang, G. Y. Zhang, X. P. Hao, B. Y. Wang, X. Q. Shen, H. Okumura, *J. Appl. Phys.* **2010**, *107*, 023528.
[71] F. A. Ponce, D. P. Bour, W. Götz, P. J. Wright, *Appl. Phys. Lett.* **1996**, *68*, 57.
[72] D. G. Zhao, D. S. Jiang, H. Yang, J. J. Zhu, Z. S. Liu, S. M. Zhang, J. W. Liang, X. Li, X. Y. Li, H. M. Gong, *Appl. Phys. Lett.* **2006**, *88*, 241917.
[73] E. R. Glaser, T. A. Kennedy, H. C. Crookham, J. A. Freitas, M. A. Khan, D. T. Olson, J. N. Kuznia, *Appl. Phys. Lett.* **1993**, *63*, 2673.
[74] E. R. Glaser, T. A. Kennedy, K. Doverspike, L. B. Rowland, D. K. Gaskill, J. A. Freitas, M. Asif Khan, D. T. Olson, J. N. Kuznia, D. K. Wickenden, *Phys. Rev. B* **1995**, *51*, 13326.
[75] M. Toth, K. Fleischer, M. R. Phillips, *Phys. Rev. B* **1999**, *59*, 1575.
[76] S. Schmult, F. Schubert, S. Wirth, A. Großer, T. Mittmann, T. Mikolajick, *J. Vacuum Sci. Technol. B, Nanotechnol. Microelectron.: Mater. Process. Measure. Phenomena* **2017**, *35*, 02B104.
[77] E. F. Schubert, I. D. Goepfert, J. M. Redwing, *Appl. Phys. Lett.* **1997**, *71*, 3224.
[78] U. Kaufmann, M. Kunzer, H. Obloh, M. Maier, C. Manz, A. Ramakrishnan, B. Santic, *Phys. Rev. B* **1999**, *59*, 5561.
[79] H. Gu, G. Ren, T. Zhou, F. Tian, Y. Xu, Y. Zhang, M. Wang, Z. Zhang, D. Cai, J. Wang, K. Xu, *J. Alloys Compd.* **2016**, *674*, 218.
[80] M. A. Reshchikov, J. D. McNamara, F. Zhang, M. Monavarian, A. Usikov, H. Helava, Y. Makarov, H. Morkoç, *Phys. Rev. B* **2016**, *94*, 035201.
[81] M. A. Reshchikov, N. M. Albarakati, M. Monavarian, V. Avrutin, H. Morkoç, *J. Appl. Phys.* **2018**, *123*, 161520.
[82] M. A. Reshchikov, A. A. Kvasov, M. F. Bishop, T. McMullen, A. Usikov, V. Soukhoveev, V. A. Dmitriev, *Phys. Rev. B* **2011**, *84*, 075212.
[83] M. A. Reshchikov, *J. Appl. Phys.* **2014**, *115*, 012010.
[84] M. A. Reshchikov, M. Vorobiov, D. O. Demchenko, U. Özgür, H. Morkoç, A. Lesnik, M. P. Hoffmann, F. Hörich, A. Dadgar, A. Strittmatter, *Phys. Rev. B* **2018**, *98*, 125207.
[85] M. A. Reshchikov, D. O. Demchenko, A. Usikov, H. Helava, Y. Makarov, *Phys. Rev. B* **2014**, *90*, 235203.
[86] J. L. Lyons, A. Alkauskas, A. Janotti, C. G. van de Walle, *Phys. Status Solidi B* **2015**, *252*, 900.
[87] A. Lesnik, M. P. Hoffmann, A. Fariza, J. Bläsing, H. Witte, P. Veit, F. Hörich, C. Berger, J. Hennig, A. Dadgar, A. Strittmatter, *Phys. Status Solidi B* **2017**, *254*, 1600708.
[88] Y. Ni, L. Li, L. He, T. Que, Z. Liu, L. He, Z. Wu, Y. Liu, *Superlattices Microstruct.* **2018**, *120*, 720.
[89] K. Fujii, T. Goto, S. Nakamura, T. Yao, *Jpn. J. Appl. Phys.* **2021**, *60*, 011002.
[90] M. A. Reshchikov, Y. T. Moon, X. Gu, B. Nemeth, J. Nause, H. Morkoç, *Phys. B: Condens. Matter* **2006**, *376–377*, 715.
[91] Y. Fang, X. Wu, J. Yang, J. Wang, Q. Wu, Y. Song, *Appl. Phys. Lett.* **2021**, *118*, 112105.
[92] F. Liang, D. Zhao, D. Jiang, Z. Liu, J. Zhu, P. Chen, J. Yang, S. Liu, Y. Xing, L. Zhang, M. Li, Y. Zhang, G. Du, *Nanomaterials* **2018**, *8*, 744.
[93] F. Zimmermann, J. Beyer, F. C. Beyer, G. Gärtner, I. Gamov, K. Irmscher, E. Richter, M. Weyers, J. Heitmann, *J. App. Phys.*, **2021**, *130*, 055703.
[94] F. Kaess, P. Reddy, D. Alden, A. Klump, L. H. Hernandez-Balderrama, A. Franke, R. Kirste, A. Hoffmann, R. Collazo, Z. Sitar, *J. Appl. Phys.* **2016**, *120*, 235705.

© 2021 The Authors. physica status solidi (a) applications and materials science published by Wiley-VCH GmbH

[95] P. Reddy, M. P. Hoffmann, F. Kaess, Z. Bryan, I. Bryan, M. Bobea, A. Klump, J. Tweedie, R. Kirste, S. Mita, M. Gerhold, R. Collazo, Z. Sitar, *J. Appl. Phys.* **2016**, *120*, 185704.
[96] A. Alkauskas, J. L. Lyons, D. Steiauf, C. G. Van de Walle, *Phys. Rev. Lett.* **2012**, *109*, 267401.
[97] M. A. Reshchikov, D. O. Demchenko, J. D. McNamara, S. Fernández-Garrido, R. Calarco, *Phys. Rev. B* **2014**, *90*, 035207.
[98] C. H. Seager, A. F. Wright, J. Yu, W. Götz, *J. Appl. Phys.* **2002**, *92*, 6553.
[99] S. Y. Karpov, *Phys. Status Solidi B* **2021**, *258*, 2100066.
[100] Y. Xu, Z. Li, X. Yang, L. Shi, P. Zhang, X. Cao, J. Nie, S. Wu, J. Zhang, Y. Feng, Y. Zhang, X. Wang, W. Ge, K. Xu, B. Shen, *Jpn. J. Appl. Phys.* **2019**, *58*, 090901.
[101] Y. Xu, X. Yang, P. Zhang, X. Cao, Y. Chen, S. Guo, S. Wu, J. Zhang, Y. Feng, F. Xu, X. Wang, W. Ge, B. Shen, *Appl. Phys. Express* **2019**, *12*, 061002.
[102] A. Kyrtsos, M. Matsubara, E. Bellotti, *Phys. Rev. B* **2016**, *93*, 245201.
[103] C. Seager, D. Tallant, J. Yu, W. Götz, *J. Lumin.* **2004**, *106*, 115.
[104] R. Armitage, Q. Yang, E. R. Weber, *J. Appl. Phys.* **2005**, *97*, 073524.
[105] M. Matsubara, E. Bellotti, *J. Appl. Phys.* **2017**, *121*, 195702.
[106] *Defects in Semiconductors, Volume 91 of Semiconductors and Semimetals* (Eds: M. A. Reshchikov, In L. Romano, V. Privitera, C. Jagadish), Elsevier, Amsterdam **2015**, pp. 315–367.
[107] J. Kang, Y. Shen, Z. Wang, *Mater. Sci. Eng.: B* **2002**, *91–92*, 303.
[108] D. O. Demchenko, I. C. Diallo, M. A. Reshchikov, *J. Appl. Phys.* **2016**, *119*, 035702.
[109] C. G. Van de Walle, C. Stampfl, J. Neugebauer, *J. Cryst. Growth* **1998**, *189–190*, 505.
[110] S. G. Christenson, W. Xie, Y. Y. Sun, S. B. Zhang, *J. Appl. Phys.* **2015**, *118*, 135708.
[111] Y. C. Chang, A. E. Oberhofer, J. F. Muth, R. M. Kolbas, R. F. Davis, *Appl. Phys. Lett.* **2001**, *79*, 281.
[112] S. Dhar, S. Ghosh, *Appl. Phys. Lett.* **2002**, *80*, 4519.
[113] S. Wu, X. Yang, Q. Zhang, Q. Shang, H. Huang, J. Shen, X. He, F. Xu, X. Wang, W. Ge, B. Shen, *Appl. Phys. Lett.* **2020**, *116*, 262101.
[114] B. Wang, F. Liang, D. Zhao, Y. Ben, J. Yang, P. Chen, Z. Liu, *Optical Express* **2021**, *29*, 3685.
[115] V. Davydov, Y. Kitaev, I. Goncharuk, A. Smirnov, J. Graul, O. Semchinova, D. Uffmann, M. Smirnov, A. Mirgorodsky, R. Evarestov, *Phys. Rev. B* **1998**, *58*, 12899.
[116] S. A. Brown, R. J. Reeves, B. Rong, R. Cheung, M. Seyboth, C. Kirchner, M. Kamp, *Nanotechnology* **2000**, *11*, 263.
[117] L. Kimerling, *Solid-State Electron.* **1978**, *21*, 1391.
[118] J.-S. Park, K. J. Chang, *Appl. Phys. Express* **2012**, *5*, 065601.
[119] K. Irmscher, I. Gamov, E. Nowak, G. Gärtner, F. Zimmermann, F. C. Beyer, E. Richter, M. Weyers, G. Tränkle, *Appl. Phys. Lett.* **2018**, *113*, 262101.
[120] I. Gamov, E. Richter, M. Weyers, G. Gärtner, K. Irmscher, *J. Appl. Phys.* **2020**, *127*, 205701.
[121] I. Levine, I. Gamov, M. Rusu, K. Irmscher, C. Merschjann, E. Richter, M. Weyers, T. Dittrich, *Phys. Rev. B* **2020**, *101*, 245205.
[122] E. E. Reuter, R. Zhang, T. F. Kuech, S. G. Bishop, *MRS Internet J. Nitride Semicond. Res.* **1999**, *4*, 363.

Johannes Heitmann holds a Ph.D. in Physics (MPI für Mikrostrukturphysik Halle 2003). Later he collected work experience in industry as Senior Engineer for Material Development at Infineon / Qimonda AG Dresden (2004–2009) and Senior Scientist at the namlab gGmbH Dresden (2009–2010). Since 2010 he is Director of the Institute for Applied Physics at the TU Bergakademie Freiberg and since 2016 he is in charge of the Fraunhofer Technolgy Center for Semiconductor Materials (THM) Freiberg. His research interests are in the field of (nano-)crystalline semiconductor materials, point defects in nitride semiconductors and high-k materials for Si and nitride electronics.

© 2021 The Authors. physica status solidi (a) applications and materials science published by Wiley-VCH GmbH